Journal of the American College of Cardiology
© 2004 by the American College of Cardiology Foundation
Published by Elsevier Inc.

Vol. 43, No. 9, 2004
ISSN 0735-1097/04/$30.00
doi:10.1016/j.jacc.2003.09.066

# Noninvasive Assessment of Ejection Intraventricular Pressure Gradients

Raquel Yotti, MD,* Javier Bermejo, MD, PHD,* J. Carlos Antoranz, PHD,†
José Luis Rojo-Álvarez, MENG, PHD,‡ Carmen Allue, RDNS,* Jacobo Silva, MD,§ M. Mar Desco, MD,‖
Mar Moreno, MD,* Miguel A. García-Fernández, MD*
*Madrid, Spain*

**OBJECTIVES** The study was designed to validate in vivo a new method to measure ejection intraventricular pressure gradients (IVPGs) by processing color M-mode Doppler data and to assess the effects of inotropic interventions on IVPGs in the clinical setting.

**BACKGROUND** In the absence of obstruction, ejection IVPGs cannot be estimated by Doppler using the simplified Bernoulli equation.

**METHODS** High-fidelity micromanometers were placed in the left ventricle of eight minipigs, and synchronic Doppler images and pressure signals were obtained during different hemodynamic conditions. Twenty healthy volunteers and 20 dilated cardiomyopathy patients were studied at baseline and during esmolol, dobutamine, and atropine infusion (only dobutamine in patients).

**RESULTS** Excellent agreement was observed between micromanometer and Doppler methods for measuring instantaneous pressure differences among the apex, the mid-cavity, and the outflow tract ($R_{intraclass}$ = 0.98, 0.81, 0.76, and 0.98 for the peak, time-to-peak, peak reverse, and time-to-peak reverse values, respectively; n = 810 beats). Error of the noninvasive method was −0.05 ± 0.25 mm Hg for the peak pressure difference. Parametrical images demonstrated that IVPGs originate mainly in the mid-ventricle and then propagate to the outflow tract. Both the magnitude and the temporal course of IVPGs were different among volunteers and patients. Inotropic interventions induced significant changes in the apex-outflow tract pressure differences in both populations, whereas atropine had no effect on IVPGs.

**CONCLUSIONS** For the first time, ejection IVPGs can be accurately visualized and measured by Doppler-echocardiography. Important aspects of the dynamic interaction among myocardial performance, load mechanics, and ejection dynamics can be assessed in the clinical setting using this method. (J Am Coll Cardiol 2004;43:1654–62) © 2004 by the American College of Cardiology Foundation

Regional ejection intraventricular pressure gradients (IVPGs) (representing the pressure field variation per unit of distance) are present within normal left ventricles (LVs), even in the absence of any anatomical obstruction (1–4). Consequently, physiological pressure differences (ΔPs) in the range of 5 to 10 mm Hg have been measured between the LV apex and the left ventricular outflow tract (LVOT) using high-fidelity micromanometers (1,4). Ejection IVPGs arise from the unsteady nature of ejective flow, from chamber geometry, and from the sequence of regional contraction (3). Therefore, ejection ΔPs are known to be related to the inotropic state and to LV size (2).

Analysis of IVPGs is of particular interest in the clinical setting. Invasive studies have demonstrated that ejection IVPGs are responsible for a significant component of systolic afterload (3). Also, IVPGs are known to be modified by myocardial diseases (5), and the analysis of ejection IVPGs has proved to be useful in characterizing ventricular performance (3,5). However, the need for sophisticated catheterization procedures has limited further research into this field.

The simplified Bernoulli equation is an accurate method to calculate intracardiac ΔPs from Doppler-derived flow-velocity measurements, but is unsuitable in the absence of a restrictive orifice (6). Ejection IVPGs are mainly inertial in origin (3), and they cannot be estimated using a formula that neglects local acceleration. Recently, we and other investigators (7–10) have demonstrated that the Euler equation can be solved from color M-mode Doppler velocity data. The present study was designed with a twofold purpose: 1) in vivo validating, against high-fidelity pressure catheters, of a new noninvasive method to measure ejection IVPGs, and 2) testing the clinical applicability of the method to evaluate the effects of drug interventions on IVPGs in healthy volunteers and in patients with dilated cardiomyopathy (DCM).

## METHODS

**Animal experimental protocol.** The animal study protocol was approved by the local Institutional Animal Care Committee. Eight minipigs (43 ± 7 kg) were used in an open-chest instrumentation setup. Animals were preanes-

From the *Department of Cardiology, §Department of Cardiovascular Surgery, and the ‖Unit of Experimental Medicine and Surgery, Hospital General Universitario Gregorio Marañón, Madrid, Spain; †Department of Mathematical Physics and Fluids, Facultad de Ciencias, Universidad Nacional de Educación a Distancia, Madrid, Spain; and the ‡Department of Signal Theory and Communications, Universidad Carlos III de Madrid, Spain. This study was presented in part at the 51st Scientific Sessions of the American College of Cardiology, Atlanta, Georgia, March 2002, and the 52nd Scientific Sessions of the American College of Cardiology, Chicago, Illinois, March 2003. This study was partially supported by the SCIT 2000–2003 Program-Contract from the Comunidad de Madrid, Spain; and by the Fondo de Investigacíon Sanitaria, Instituto Carlos III, Madrid, Spain (Project Number PI031220).

Manuscript received May 20, 2003; revised manuscript received August 14, 2003, accepted September 29, 2003.

**Abbreviations and Acronyms**

| | |
|---|---|
| ΔP | = ejection intraventricular pressure difference |
| DCM | = dilated cardiomyopathy |
| ECG | = electrocardiogram/electrocardiographic |
| IVPG | = intraventricular pressure gradient |
| LV | = left ventricle/ventricular |
| LVOT | = left ventricular outflow tract |
| $R_{intraclass}$ | = intraclass correlation coefficient |

thetized with ketamine and xylazine, and then mechanically ventilated. Complete anesthesia and relaxation during the experiment were obtained by repetitive boluses of pentobarbital (15 mg/kg intravenous + 5 mg/kg/15 min) and pancuronium (0.2 mg/kg). Blood gases were measured at 15- to 30-min intervals, and the ventilator was adjusted accordingly. Once experiments were completed, animals either were euthanized or underwent subsequent unrelated experimental procedures.

The heart was exposed by median sternotomy without opening the pericardium and cradled to obtain a suitable ultrasonic window. For load manipulation, a snare was placed around the inferior vena cava, and a 20-mm valvuloplasty balloon was advanced to the infrarenal aorta. A pacing electrode was sutured to the right atrial appendage, and a needle micromanometer (Millar Instruments, Houston, Texas) was inserted epicardially inside the apex. A dual-micromanometer catheter (3-cm sensor spacing, Millar Instruments) was inserted retrogradely into the LV from the ascending aorta, placing the proximal sensor at the LVOT and the distal sensor in the mid-cavity. Micromanometers were prepared, balanced, and calibrated according to the manufacturer's specifications. To avoid drift and eliminate hydrostatic ΔPs (3), micromanometers were also balanced in vivo during a long diastasis following a premature beat. To ensure temporal matching of Doppler-echocardiography and pressure data, a synchronicity signal was simultaneously connected to the ultrasound scanner and the signal acquisition system. Pressure, synchronicity, and electrocardiographic (ECG) signals were digitized at 500 Hz on a Pentium III computer using custom-built amplifiers, a 16-channel A-D converter board (Keithley Instruments, Cleveland, Ohio), and virtual instrumentation software (Testpoint, Capital Equipment, Billerica, Massachusetts).

Each animal was studied at baseline and at four hemodynamic states: 1) esmolol (bolus 500 μg/kg, followed by 50 to 200 μg/kg/min in steps of 50 μg/kg/min every 10 min); 2) dobutamine (up to 10 μg/kg/min); and atrial pacing at: 3) 120 beats/min, and 4) 150 beats/min. In each state, data sets were acquired once hemodynamics were stable at baseline, during cava, and during aortic occlusion. Three consecutive beats were recorded during end-expiration apnea from each state-load condition.

**Human population and clinical protocol.** Twenty healthy volunteers and 20 DCM patients were studied. Volunteers were not on any medication, and cardiovascular disease was ruled out by history, clinical examination, ECG, and Doppler-echocardiography. Inclusion criteria for DCM patients were: 1) ejection fraction <30%, 2) LV volumes >2 SD normal values for age and gender, and 3) sinus rhythm. Patients with a functional class IV or prior history of sustained ventricular tachycardia were not included. In volunteers, esmolol and dobutamine (same doses as in the animal protocol) were infused, followed by atropine (0.3-mg boluses) titrated to match dobutamine heart rate. Recordings were obtained during a steady hemodynamic state, and each drug was followed by a 30-min washout period. In DCM patients, only dobutamine was infused. The study protocol was approved by the institutional ethical committee, and written informed consent was obtained from all subjects.

**Echocardiographic image acquisition and analysis.** A 2.0 to 3.5-MHz transducer was used on a Sequoia C-256 system (Siemens AG, Munich, Germany). Images were obtained from a posteriorly modified five-chamber apical view, using an epicardial (animals) and a transthoracic (humans) approach. Special care was taken to align the M-mode cursor with the ejective flow, visualized by two-dimensional color Doppler. Horizontal sweep was set to 150 or 200 mm/s. End-diastolic and end-systolic dimensions, shortening fraction, and LV stroke volume were calculated in the clinical study from standard M-mode, two-dimensional, and Doppler spectrograms as recommended (11).

The general method used for digital image processing of color M-mode Doppler echocardiograms has been described elsewhere (10). Briefly, if the M-mode cursor closely approximates a flow streamline, the spatio-temporal velocity distribution of a discrete blood sample is provided by the value of its corresponding pixel color: $v(s,t)$, where $v$ represents velocity, $s$ represents the linear dimension of the streamline, and $t$ is time. Thus, the color M-mode Doppler recording provides the data necessary to solve Euler's momentum equation:

$$\frac{\delta p}{\delta s} = -\rho \cdot \left( \frac{\delta v}{\delta t} + v \cdot \frac{\delta v}{\delta s} \right)$$

where $p$ designates pressure and $\rho$ represents blood density. The first term in the right side of the equation designates inertial (local) acceleration, whereas the second term accounts for convective (spatial) acceleration.

Calibration and Doppler scale limits were automatically read from the image. The onset of the QRS was manually identified and defined as $t = 0$. Velocity was decoded, dealiased, and fitted to a tensor-product smoothing spline (smoothing parameter p = 0.004) (10). Next, partial derivatives of the velocity data were calculated as the analytical first derivative of each polynomial piece. Ejection IVPGs were displayed as color overlays representing the ΔP between one pixel and another one located 1 cm closer to the ultrasound transducer in mm Hg/cm (Fig. 1). The locations of the LV apex and the LVOT were visually traced in the

JACC Vol. 43, No. 9, 2004
May 5, 2004:1654–62

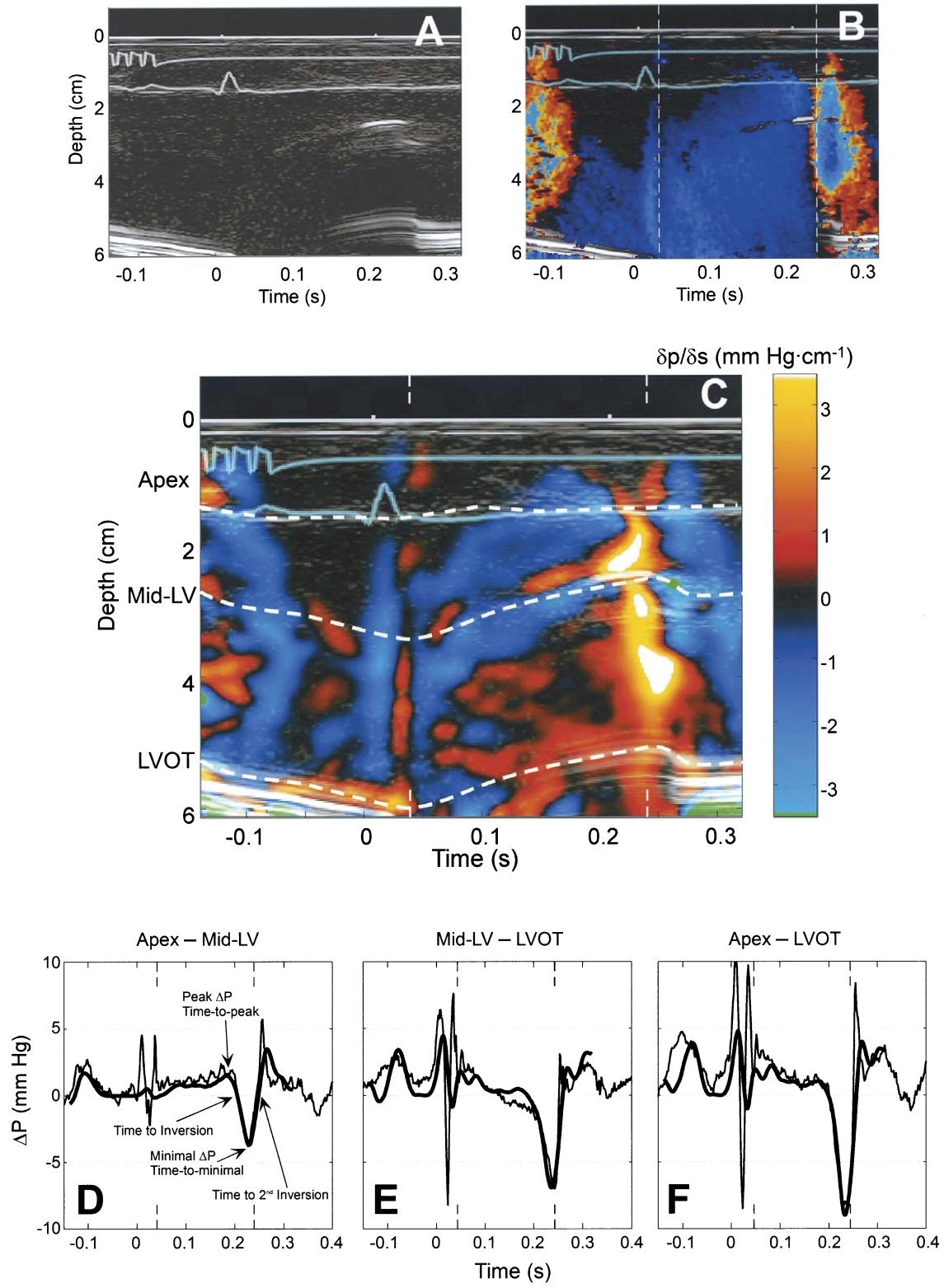


**Figure 1.** Validation example from a swine experiment. **(A)** Greyscale M-mode recording. The electrocardiogram **(bottom)** and synchronicity **(top)** signals are shown. Micromanometer echoes are visualized in the mid-cavity and left ventricular outflow tract (LVOT), and were confirmed by two-dimensional sequences acquired simultaneously. **(B)** Raw color M-mode Doppler image. **(C)** Parametrical intraventricular pressure gradient (IVPG) (δp/δs) image overlay on the greyscale figure of **A.** The sign and magnitude of the gradient is given by the **color bar,** representing the ejection intraventricular pressure difference (ΔP) between each pixel and another one located 1 cm closer to the transducer. The equivalent location of the three micromanometers in this IVPG field has been traced **(dashed lines)**. **(D, E, and F)** The ΔP curves between the sensor locations represented in **C,** obtained by micromanometers **(thin lines)** and by Doppler-echocardiography **(thick lines)**. Ejection onset and end are shown **(dashed lines in B and ticks in C to F)**. Curve parameters analyzed in the present study are displayed in **D.**

greyscale image layer, attempting to match instantaneous micromanometer positions (Fig. 1). The distance between the mid-LV and LVOT micromanometers was measured from two-dimensional echocardiographic sequences obtained at the beginning of each acquisition (slightly less than nominal separation due to catheter bending, approximately 2.6 to 2.8 cm apart). Discrete ΔPs were calculated by spatial integration of IVPG maps between each pair of stations, providing three validation ΔP curves from each IVPG image. In the clinical study, the apical–LVOT ΔP was calculated.

Intra- and interobserver reproducibility (30 beats from the clinical data set, blindly measured >3 months apart) of peak ejection ΔP were 0.1 ± 1.2 ($R_{intraclass}$ = 0.93) and 0.2 ± 1.0 mm Hg ($R_{intraclass}$ = 0.95), respectively, where $R_{intraclass}$ represents the intraclass correlation coefficient.

**Pressure difference curve analysis.** The ΔP curves between apex–LVOT, apex–mid-cavity, and mid-cavity–LVOT were calculated offline by subtraction of the respective simultaneous pressure tracings. To ensure the analysis of the same beat, the temporal offset between Doppler-echocardiography and invasive data sets was obtained by cross-correlation of their synchronicity signals. The onset and the end of the ejection period were identified from the raw color-Doppler recordings as the beginning and the end of flow across the aortic valve. The following ΔP parameters were blindly obtained for each technique, constrained to the ejection period: peak and time-to-peak, minimal and time-to-minimal, time to ΔP inversion, and time to second inversion (slightly after end ejection). In the clinical study, both the value and the time of peak IVPG were also measured from the parametrical map. Temporal parameters were normalized to ejection duration in the clinical study.

**Statistical analysis.** The validation analysis was performed on a single-beat basis, whereas results of three consecutive cycles were averaged in the clinical study. Quantitative variables are expressed as the mean ± SD. The agreement between techniques was assessed calculating the mean ± SD of error, Bland-Altman charts, and the intraclass correlation coefficient ($R_{intraclass}$). In the clinical study, differences among phases were assessed by analysis of variance accounting for repeated-measures, followed by Dunnet's contrasts. Unpaired *t* tests were used for comparisons between healthy volunteers and patients. Variables related to peak ΔP were assessed calculating Pearson's correlation coefficients, followed by multivariate linear regression analysis with variable selection based on Alkaike's AIC criterion. A p value <0.05 was considered to be significant.

## RESULTS

**Experimental validation.** A total of 810 beats were analyzed. Peak baseline ejection ΔPs were 0.7 ± 0.2, 2.5 ± 1.5, and 2.9 ± 1.7 mm Hg, for the apex–mid-LV, mid-LV–LVOT, and apex–LVOT locations, respectively. The ΔP curves obtained by Doppler-echocardiography closely matched invasive signals, and a low-pass filter effect was observed in noninvasive tracings (Fig. 1). The accuracy of Doppler-echocardiography ΔP curve parameters was excellent (Table 1, Fig. 2). Beat-to-beat variability (animal data set, baseline states of all phases, n = 66, three consecutive beats) for peak ejection ΔP values was 0.6 ± 0.5 and 0.5 ± 0.5 mm Hg, for Doppler-echocardiography and micromanometer methods, respectively. The phase lag between methods was 7 ± 25 ms. Ejection ΔPs adopted a characteristic configuration (Figs. 1 and 3) showing an early peak, a slow decrease, a mid-late ejection ΔP reversal, and, finally, a late reverse peak. Ejection IVPGs were caused mainly by inertial forces, whereas convective ΔP curves did not resemble micromanometer tracings (Fig. 3).

**Pressure gradients in volunteers and DCM patients.** There were no adverse drug effects, and recordings suitable for processing were obtained from all subjects. The highest IVPGs originated between the mid-cavity and the LVOT (Figs. 4 and 5). Patients showed a number of characteristics different from normal subjects: lower peak IVPG, lower peak ΔP, and lower peak-reverse ΔP values, mainly due to lower convective forces. The time to peak ΔP and the time to ΔP inversion occurred earlier during ejection in DCM patients than in normal subjects, whereas the time to second inversion occurred later. Dobutamine significantly increased all absolute values of IVPG and ΔP. Conversely, peak positive values were decreased by esmolol in normal subjects. Atropine did not modify either IVPG or ΔP parameters (Table 2). Peak ΔPs correlated with heart rate, systolic blood pressure, and, most significantly, with stroke volume (Table 3).

## DISCUSSION

The present study demonstrates, for the first time in hearts without intraventricular obstruction, that ejection IVPGs can be accurately measured using Doppler-echocardiography. The clinical study illustrates the applicability of this technique and provides new spatio-temporal maps of the distribution of IVPG within the normal and DCM human ventricles.

**Pressure gradients assessed by color M-mode Doppler.** The possibility of calculating intracardiac ΔPs from color M-mode Doppler images was first demonstrated by Greenberg et al. (7). By solving the unsteady Bernoulli equation, these investigators accurately measured diastolic ΔPs across a normal mitral valve in an open-chest animal model (7), and in patients undergoing coronary artery bypass grafting (9). Later, the same group validated a method for estimating diastolic intraventricular ΔPs, based on the solution of the Euler equation (8). Our method, proposed almost simultaneously (10), introduces some potential improvements. First, velocity derivatives are solved analytically, increasing the robustness of mathematical calculations. Second, the effects of cardiac translation can be partially corrected by

**Table 1.** Agreement Between Parameters of Ejection Pressure Difference Curves Obtained by Micromanometers and by Doppler-Echocardiography

| | Absolute Error (mm Hg or ms) | Relative Error (%) | $R_{intraclass}$ | SEE (mm Hg or ms) |
|---|---|---|---|---|
| Peak ejection ΔP (mm Hg) | | | | |
| All locations | −0.05 ± 0.25 | −3 ± 14 | 0.98 | 0.25 |
| Apex–mid-cavity | −0.07 ± 0.18 | −8 ± 21 | 0.89 | 0.17 |
| Mid-cavity–LVOT | −0.03 ± 0.25 | −2 ± 13 | 0.97 | 0.25 |
| Apex–LVOT | −0.06 ± 0.30 | −2 ± 12 | 0.97 | 0.29 |
| Peak reverse ΔP (mm Hg) | | | | |
| All locations | 0.68 ± 1.51 | −19 ± −42 | 0.76 | 1.45 |
| Apex–mid-cavity | 1.19 ± 16.26 | −56 ± −90 | 0.29 | 1.62 |
| Mid-cavity–LVOT | 0.01 ± 1.24 | 0 ± −35 | 0.72 | 1.01 |
| Apex–LVOT | 1.29 ± 1.39 | −26 ± −28 | 0.66 | 1.36 |
| Time to peak ejection ΔP (ms) | | | | |
| All locations | 9 ± 20 | 8 ± 19 | 0.81 | 19 |
| Apex–mid-cavity | 15 ± 30 | 13 ± 25 | 0.71 | 27 |
| Mid-cavity–LVOT | 4 ± 14 | 4 ± 14 | 0.89 | 14 |
| Apex–LVOT | 9 ± 15 | 9 ± 14 | 0.83 | 13 |
| Time to ΔP reversal (ms) | | | | |
| All locations | 16 ± 41 | 8 ± 19 | 0.73 | 37 |
| Apex–mid-cavity | 8 ± 42 | 4 ± 20 | 0.69 | 39 |
| Mid–cavity-LVOT | 18 ± 42 | 8 ± 19 | 0.73 | 38 |
| Apex–LVOT | 20 ± 38 | 9 ± 17 | 0.75 | 34 |
| Time to peak reverse ΔP (ms) | | | | |
| All locations | 1 ± 10 | 0 ± 3 | 0.98 | 10 |
| Apex–mid-cavity | 1 ± 14 | 0 ± 5 | 0.97 | 13 |
| Mid-cavity–LVOT | 2 ± 8 | 1 ± 2 | 0.99 | 8 |
| Apex–LVOT | 1 ± 9 | 0 ± 3 | 0.99 | 8 |

ΔP = ejection intraventricular pressure difference; LVOT = left ventricular outflow tract; $R_{intraclass}$ = intraclass correlation coefficient; SEE = standard error of the estimate of the regression slope.

manually locating the measuring stations throughout the entire sequence. And third, not only ΔP curves, but also parametric IVPGs images are provided, showing the spatio-temporal distribution of intracardiac pressure forces. We believe this type of representation provides useful information. A previous study (2) and ours demonstrate that about 25% to 30% of ejection IVPGs hold between the apex and the mid-cavity stations. These apical ejection IVPGs have never been characterized in humans, and can now be visualized and measured with reasonable accuracy (Table 1, Figs. 4 and 5).

A number of implicit assumptions are present in Euler's one-dimensional simplification of ejection flow-dynamics: 1) viscous frictional effects are neglible in the ejection field and confined to very thin boundary layers; 2) the main core of LV outflow is irrotational; and 3) there is an absence of

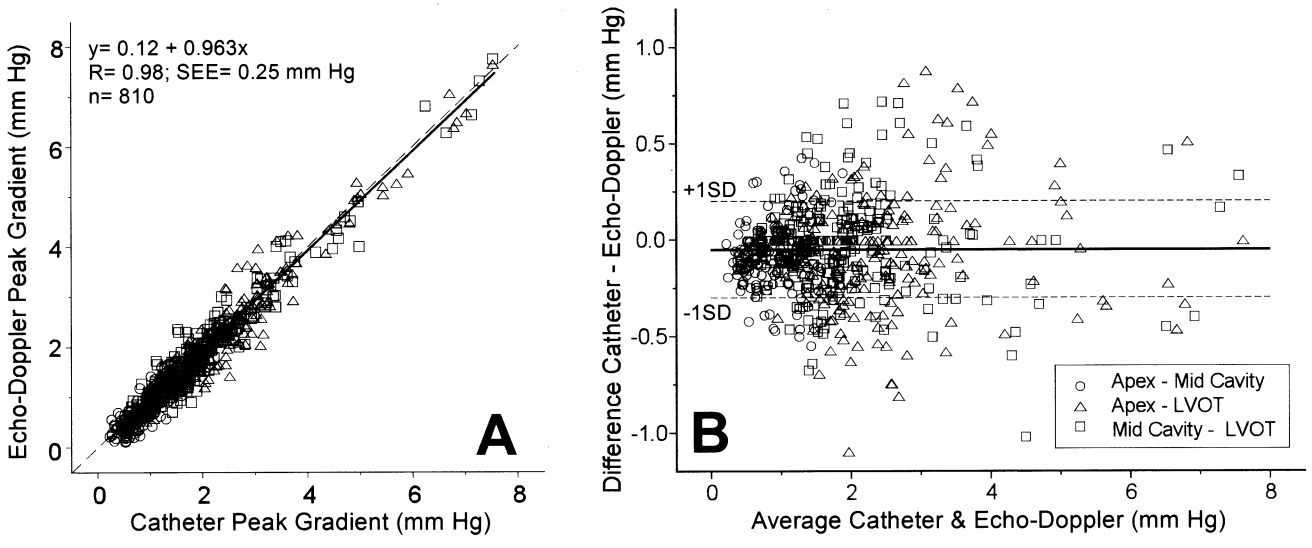


**Figure 2.** Correlation **(A)** and Bland-Altman **(B)** plots of the agreement between noninvasive and micromanometer measurements of peak ejection intraventricular pressure difference. LVOT = left ventricular outflow tract.

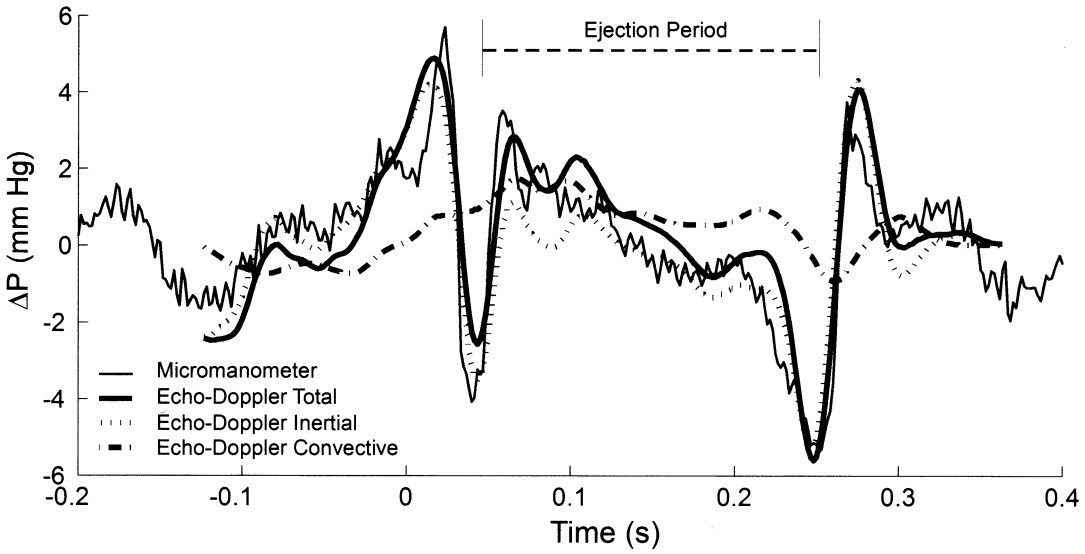


**Figure 3.** Predominant contribution of inertial over convective forces to total interventricular pressure gradient. ΔP = ejection interventricular pressure difference.

vorticity in the LV ejection flow. These mechanical aspects of ventricular ejection, to date incompletely addressed in vivo (12), are supported by our validation results.

Methods based on solving fluid-dynamic differential equations, such as the one we propose, are accurate to calculate regional differences of pressure within and between the cardiac chambers. Absolute local pressure curves can only be inferred if instantaneous pressure at a given position is either known or assumed. Furthermore, to obtain absolute pressure from flow velocity accurately, not only local but also global inertial forces (those required to accelerate the total blood within the ventricle) would also have to be accounted for (5,13).

**Ejection IVPGs in health and disease.** Laszt and Müller described the existence of ejection intraventricular regional ΔPs more than 50 years ago (14). However, ejection ΔPs could not be well characterized until the introduction of high-fidelity solid-state pressure catheters (15). With this tool, ejection intraventricular ΔPs were described in dogs, and the relationship with myocardial contractility was suggested (2). Also, intraventricular ejection ΔPs were studied invasively in a small number of normal subjects (1). Remarkably, both the magnitude and the shape of ΔP curves obtained in our study are identical to the micromanometer tracings provided by these studies (1,3). Although intraventricular ΔPs have never been analyzed in humans undergoing pharmacological interventions, our findings agree with previous invasive animal studies: peak ejection ΔPs are increased by beta-agonists (2,16), and reduced by beta-blocking agents (2,16).

Invasive assessment of intraventricular ΔPs has helped clarify the hemodynamics of obstructive and nonobstructive forms of hypertrophic cardiomyopathy (4). In aortic valve stenosis, ejection intraventricular ΔPs are responsible for about half the total transvalvular ΔP, and they are a major determinant of cardiac output (17,18). However, to our knowledge, ejection intraventricular ΔPs have never been studied invasively in patients with DCM. Isaaz and Pasipoularides (5) used a noninvasive method to derive ejection ΔPs from manually digitized pulsed-wave Doppler spectrograms in patients with DCM. Their study also demonstrated that, although theoretically greater disproportion between the mid-LV and the LVOT should increase convective IVPGs in dilated ventricles (3), reduced ejection velocities due to systolic dysfunction cause convective forces to be lower than in normal hearts (5). For this reason, the time to ΔP reversal should take place earlier in DCM than in normal subjects. Our results in the DCM population are fully concordant with these observations (Table 2).

**Clinical applications.** The estimation of systolic IVPGs has important implications for the assessment of ventricular load. Our study validates a new noninvasive method to quantify intrinsic afterload (19) by Doppler-echocardiography. The results of our and previous studies (2,5) indicate that the intrinsic load adds about 10% to the extrinsic load in normal subjects, a value that is close to the oscillatory component of aortic input impedance. Interestingly, the oscillatory component of longitudinal intraventricular systolic impedance can also be assessed using our method, and preliminary results suggest it might not be negligible (20).

The use of the temporal derivative of LV pressure (dP/dt) as an index of myocardial contractility is based on the diagnostic value of initial impulsive forces (21). A computer fluid-dynamic simulation has suggested a theoretical advantage of peak intraventricular ΔP and flow acceleration over peak dP/dt (22). Flow acceleration has recently been shown to provide a robust estimator of peak systolic elastance (23). Similarly, the analysis of ejection IVPGs may be helpful to assess contractility (24).

JACC Vol. 43, No. 9, 2004
May 5, 2004:1654–62

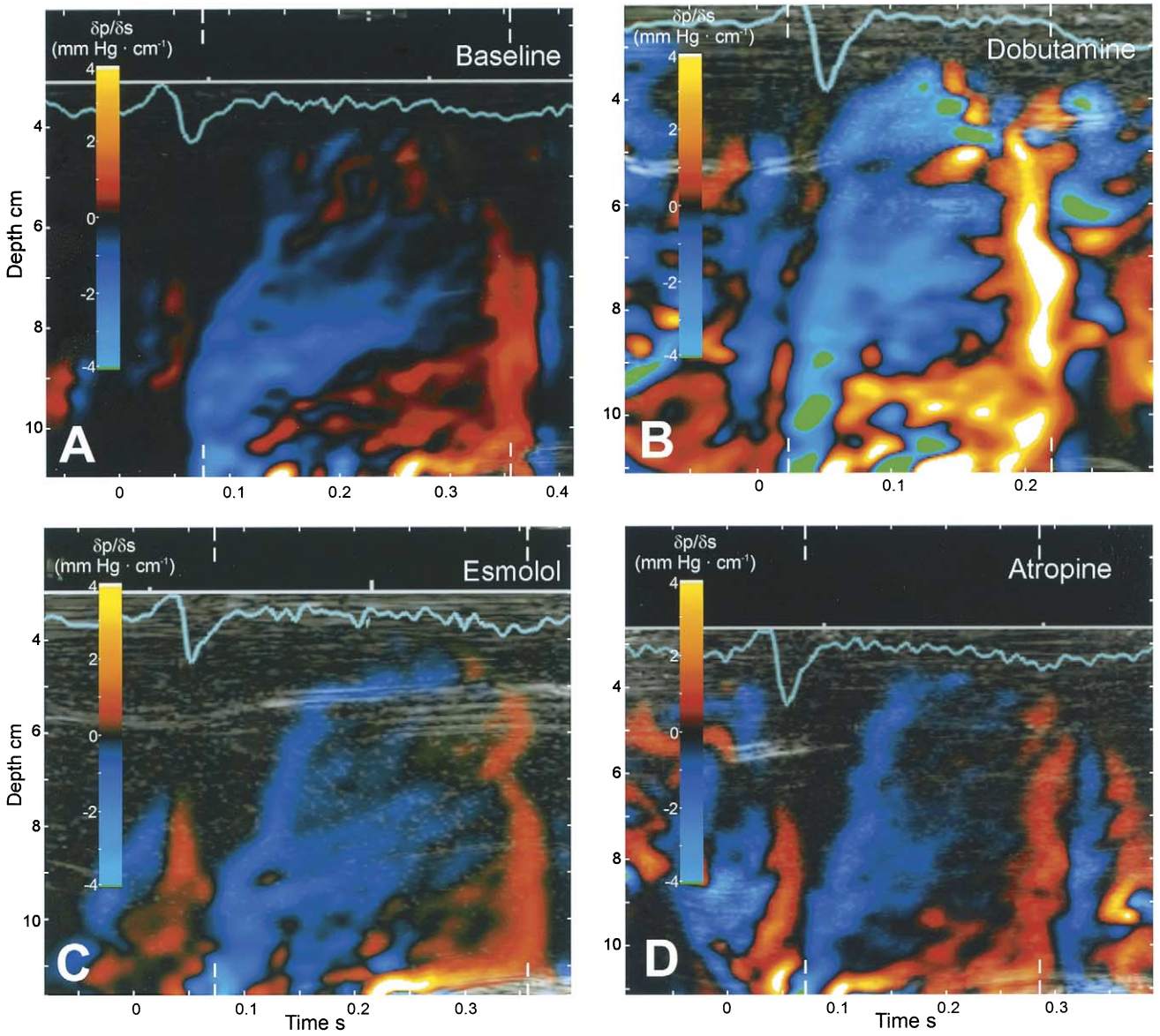


**Figure 4.** Effects of inotropic interventions on interventricular pressure gradients (IVPGs) in a healthy volunteer. Ejection IVPG images obtained at baseline **(A),** during dobutamine **(B),** esmolol **(C),** and atropine **(D)** infusion. **White ticks** represent ejection onset and end. In the **color scale** used for visualization, IVPGs above and below the scale limits (±4 mm Hg/cm) are displayed in **white** and **green,** respectively. A fixed color scale for all panels has been used to allow a visual comparison among phases as well as with images in Figure 5.

Reversed ΔP during late ejection is the consequence of the kinetic energy of blood due to the momentum imparted to it earlier in systole (21,25). As shown in our study (Figs. 1, 3, and 4), negative ejection gradients hold up to the isovolumic relaxation period. During isovolumic relaxation a negative (suction) ΔP has been described between the LV apex and the LVOT (26). Therefore, the temporal extent of diastolic-reversed IVPGs could be useful to determine the rate of myocardial relaxation (24).

**Study limitations.** Ejection velocities measured using Doppler represent the combination of intraventricular acceleration within the heart, plus the effect of ventricular translation within the chest. Because these two components are of opposite direction, Doppler-derived velocities are lower than net intraventricular velocities (27). Although this would lead to underestimation of inertial acceleration, it has been recently demonstrated that longitudinal displacement of the center of mass of the LV is in the range of ±5 cm/s (28). Therefore, we believe this effect should not lead to significant inaccuracy either in open or in closed-chest setups.

A second potential limitation is that the validation study was not performed in humans, owing to the need of multisite micromanometer instrumentation. Because geometrical properties of the pig's LV closely resemble those of humans, we do not anticipate relevant species-related differences. A third limitation is related to LV outflow profile.

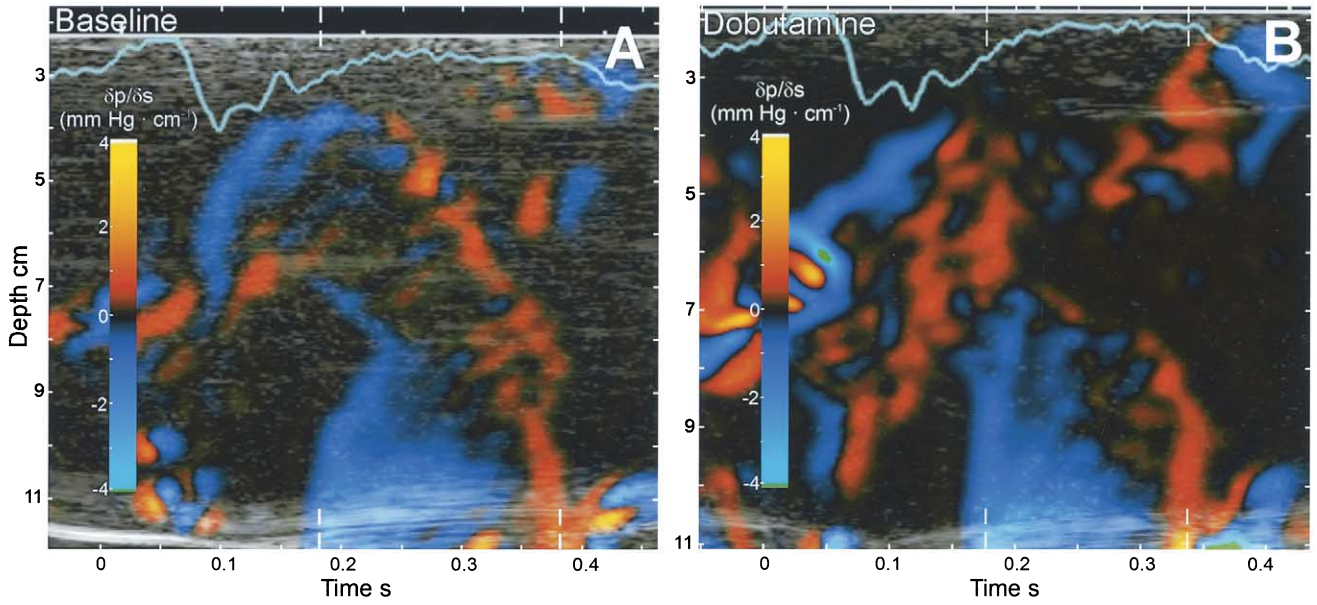


**Figure 5.** Ejection interventricular pressure gradient (IVPG) in a patient with dilated cardiomyopathy. Images were obtained at baseline **(A)** and during dobutamine infusion **(B).** Notice the differences in magnitude, spatial, and temporal extent of ejection IVPGs as compared to Figure 4.

In this study, outflow velocities were obtained across the center of the LVOT. However, it is known that outflow velocity is slightly skewed (29). According to Euler's equation, regional variations in outflow profile should modify flow velocities and IVPGs in parallel. For this reason, special care was taken in the study to match micromanometer and echo-Doppler measuring stations. Nevertheless, the skewed outflow profile must be recognized as a source of limited consistency and reproducibility of all methods that measure ejection IVPGs. Finally, healthy volunteers and DCM patient groups were not matched for age; the comparison of hemodynamic findings between both groups should therefore be interpreted with caution.

**Conclusions.** This study validates, for the first time, a fully noninvasive method to assess the dynamic interaction among myocardial performance, load mechanics, and intraventricular fluid dynamics in the clinical setting. Although the method is based on offline processing of digital color M-mode Doppler images, it could be incorporated into the analysis software of future ultrasound scanners.

**Table 2.** Results of the Clinical Study Showing Clinical, Hemodynamic, and Ejection IVPG Data From Healthy Volunteers (n = 20) and Patients With DCM (n = 20)

| | Healthy Volunteers | | | | DCM | |
|---|---|---|---|---|---|---|
| | **Baseline** | **Esmolol** | **Dobutamine** | **Atropine** | **Baseline** | **Dobutamine** |
| Age (yrs) | 29 ± 1 | | | | 62 ± 2† | |
| Gender (M/F) | 10/10 | | | | 14/6 | |
| Weight (kg) | 69 ± 1 | | | | 68 ± 3 | |
| Left bundle branch block (n) | 0 | | | | 8† | |
| Heart rate (beats/min) | 72 ± 2 | 64 ± 1 | 92 ± 3* | 95 ± 3* | 79 ± 3 | 92 ± 4* |
| Shortening fraction (%) | 41 ± 1 | 34 ± 1* | 53 ± 2* | 41 ± 1 | 14 ± 1† | 21 ± 2*† |
| LV end-diastolic diameter (mm) | 46 ± 6 | 47 ± 5 | 48 ± 5 | 46 ± 5 | 64 ± 8† | 64 ± 9† |
| Systolic blood pressure (mm Hg) | 117 ± 3 | 105 ± 2* | 139 ± 4* | 117 ± 2 | 112 ± 5 | 125 ± 7 |
| Ejection onset (ms after QRS onset) | 69 ± 15 | 77 ± 15 | 38 ± 14* | 71 ± 15 | 130 ± 46† | 100 ± 44*† |
| Ejection duration (ms) | 279 ± 20 | 280 ± 23 | 220 ± 21* | 249 ± 23* | 219 ± 35† | 203 ± 29*† |
| Ejection IVPG data | | | | | | |
| Peak ejection IVPG (mm Hg/cm) | 3.3 ± 1.6 | 2.0 ± 0.7* | 6.1 ± 2.6* | 2.6 ± 0.9 | 2.1 ± 0.8† | 3.2 ± 1.1*† |
| Peak ΔP (mm Hg) | 4.7 ± 1.3 | 4.0 ± 1.7* | 9.5 ± 2.2* | 4.2 ± 1.3 | 3.6 ± 1.1† | 5.4 ± 2.1*† |
| Minimal ΔP (mm Hg) | −4.0 ± 0.8 | −3.8 ± 1.0 | −10.1 ± 4.8* | −4.8 ± 1.1 | −2.4 ± 0.9† | −3.4 ± 1.7*† |
| Peak inertial ΔP (mm Hg) | 3.7 ± 1.4 | 3.0 ± 1.3 | 6.6 ± 1.8* | 3.2 ± 1.3 | 3.3 ± 1.0 | 4.9 ± 1.8*† |
| Peak convective ΔP (mm Hg) | 2.6 ± 0.9 | 2.1 ± 1.4 | 5.2 ± 1.5* | 2.0 ± 0.8 | 1.3 ± 0.7† | 2.2 ± 0.9*† |
| Time to peak IVPG (% ejection) | 18 ± 10 | 11 ± 9 | 21 ± 14 | 11 ± 10 | 8 ± 9† | 12 ± 10* |
| Time to peak ΔP (% ejection) | 10 ± 6 | 12 ± 5 | 9 ± 3 | 9 ± 12 | 5 ± 4† | 7 ± 5 |
| Time to ΔP inversion (% ejection) | 68 ± 6 | 68 ± 8 | 69 ± 8 | 60 ± 27 | 51 ± 14† | 55 ± 13† |
| Time to 2nd ΔP inversion (ms after end-ejection) | 20 ± 5 | 23 ± 6 | 12 ± 6 | 13 ± 5 | 29 ± 14† | 28 ± 17† |

*$p < 0.05$ versus baseline. †$p < 0.05$ DCM patients versus healthy volunteers.
DCM = dilated cardiomyopathy; IVPG = ejection intraventricular pressure gradient; other abbreviations as in Table 1.

**Table 3.** Factors Related to the Peak Intraventricular Pressure Difference in the Clinical Study

| | Univariate | Multivariate | | |
|---|---|---|---|---|
| Variable | R | b | $\beta$ | p Value |
| Heart rate | 0.26 | 0.04 | 0.22 | 0.007 |
| Systolic blood pressure | 0.40 | 0.02 | 0.20 | 0.02 |
| Diastolic blood pressure | −0.02 | | | |
| LV end-diastolic dimension | −0.13 | | | |
| LV end-systolic dimension | −0.26 | | | |
| LV shortening fraction | 0.38 | | | |
| LV stroke volume | 0.50 | 0.08 | 0.47 | <0.001 |

Pooled data from all inotropic states in 20 healthy volunteers and 20 dilated cardiomyopathy patients (n = 120).

b = regression coefficient; $\beta$ = standardized regression coefficient; LV = left ventricular; R = Pearson's correlation coefficient. Adjusted $R^2$ for the multivariate model = 0.36.

## Acknowledgments

We are indebted to all personnel from the Unit of Experimental Medicine and Surgery and from the Laboratory of Echocardiography of the Hospital General Universitario Gregorio Marañón for their assistance in data acquisition.

**Reprint requests and correspondence:** Dr. Javier Bermejo, Laboratory of Echocardiography, Department of Cardiology, Hospital General Universitario Gregorio Marañón, Dr. Esquerdo 46, 28007 Madrid, Spain. E-mail: javbermejo@jet.es.

## REFERENCES

1. Pasipoularides A, Murgo JP, Miller JW, Craig WE. Nonobstructive left ventricular ejection pressure gradients in man. Circ Res 1987;61: 220–7.
2. Falsetti HL, Verani MS, Chen CJ, Cramer JA. Regional pressure differences in the left ventricle. Cathet Cardiovasc Diagn 1980;6:123–34.
3. Pasipoularides A. Clinical assessment of ventricular ejection dynamics with and without outflow obstruction. J Am Coll Cardiol 1990;15: 859–82.
4. Murgo JP, Alter BR, Dorethy JF, Altobelli SA, McGranahan GM Jr. Dynamics of left ventricular ejection in obstructive and nonobstructive hypertrophic cardiomyopathy. J Clin Invest 1980;66:1369–82.
5. Isaaz K, Pasipoularides A. Noninvasive assessment of intrinsic ventricular load dynamics in dilated cardiomyopathy. J Am Coll Cardiol 1991;17:112–21.
6. Hatle L, Brubakk A, Toromsdal A, Angelsen B. Noninvasive assessment of pressure drop in mitral stenosis by Doppler ultrasound. Br Heart J 1978;43:131–5.
7. Greenberg NL, Vandervoort PM, Thomas JD. Instantaneous diastolic transmitral pressure differences from color Doppler M-mode echocardiography. Am J Physiol 1996;271:H1267–76.
8. Greenberg NL, Vandervoort PM, Firstenberg MS, Garcia MJ, Thomas JD. Estimation of diastolic intraventricular pressure gradients by Doppler M-mode echocardiography. Am J Physiol 2001;280: H2507–15.
9. Firstenberg MS, Vandervoort PM, Greenberg NL, et al. Noninvasive estimation of transmitral pressure drop across the normal mitral valve in humans: importance of convective and inertial forces during left ventricular filling. J Am Coll Cardiol 2000;36:1942–9.
10. Bermejo J, Antoranz JC, Yotti R, Moreno M, Garcia-Fernandez MA. Spatio-temporal mapping of intracardiac pressure gradients. A solution to Euler's equation from digital postprocessing of color Doppler M-mode echocardiograms. Ultrasound Med Biol 2001;27:621–30.
11. Quinones MA, Otto CM, Stoddard M, Waggoner A, Zoghbi WA. Recommendations for quantification of Doppler echocardiography: a report from the Doppler Quantification Task Force of the Nomenclature and Standards Committee of the American Society of Echocardiography. J Am Soc Echocardiogr 2002;15:167–84.
12. Pasipoularides A, Murgo JP, Bird JJ, Craig WE. Fluid dynamics of aortic stenosis: mechanisms for the presence of subvalvular pressure gradients. Am J Physiol 1984;246:H542–50.
13. Isaaz K. Expanding the frontiers of Doppler echocardiography for the noninvasive assessment of diastolic hemodynamics. J Am Coll Cardiol 2000;36:1950–2.
14. Laszt L, Müller A. Über den Druckverlauf im linken Ventrikel und Vorhof und in der Aorta ascendens. Hel Physiol Acta 1951;9:55–73.
15. Murgo JP, Altobelli SA, Dorethy JF, Logsdon JR, McGranahan GM, Normal ventricular ejection in man during rest and exercise. Physiologic principles of heart sounds and murmur. Am Heart Assoc Monogr 1975;46:92–101.
16. Butler CK, Wong AY, Armour JA. Systolic pressure gradients between the wall of the left ventricle, the left ventricular chamber, and the aorta during positive inotropic states: implications for left ventricular efficiency. Can J Physiol Pharmacol 1988;66:873–9.
17. Bird JJ, Murgo JP, Pasipoularides A. Fluid dynamics of aortic stenosis: subvalvular gradients without subvalvular obstruction. Circulation 1982;66:835–40.
18. Laskey WK, Kussmaul WG. Subvalvular gradients in patients with valvular aortic stenosis: prevalence, magnitude, and physiological importance. Circulation 2001;104:1019–22.
19. Shim Y, Hampton TG, Straley CA, et al. Ejection load changes in aortic stenosis. Observations made after balloon aortic valvuloplasty. Circ Res 1992;71:1174–84.
20. Rojo JL, Bermejo J, Yotti R, et al. Non-invasive assessment of ejection left ventricular longitudinal impedance by image postprocessing of color-Doppler M-mode echocardiograms (abstr). Circulation 2001; 104 Suppl II:751.
21. Rushmer RF. Initial ventricular impulse: a potential key to cardiac evaluation. Circulation 1964;29:268–83.
22. Redaelli A, Montevecchi FM. Intraventricular pressure drop and aortic blood acceleration as indices of cardiac inotropy: a comparison with the first derivative of aortic pressure based on computer fluid dynamics. Med Eng Phys 1998;20:231–41.
23. Bauer F, Jones M, Shiota T, et al. Left ventricular outflow tract mean systolic acceleration as a surrogate for the slope of the left ventricular end-systolic pressure-volume relationship. J Am Coll Cardiol 2002; 40:1320–7.
24. Yotti R, Bermejo J, Antoranz JC, et al. Noninvasive assessment of ventricular relaxation and contractility indices by analysis of intraventricular ejection pressure-gradient curves derived from Doppler echocardiography (abstr). J Am Coll Cardiol 2003;41 Suppl A:447A.
25. Noble MI. The contribution of blood momentum to left ventricular ejection in the dog. Circ Res 1968;23:663–70.
26. Steine K, Stugaard M, Smiseth O. Mechanisms of diastolic intraventricular regional pressure differences and flow in the inflow and outflow tracts. J Am Coll Cardiol 2002;40:983–90.
27. Cao T, Shapiro SM, Bersohn MM, Liu SC, Ginzton LE. Influence of cardiac motion on Doppler measurements using in vitro and in vivo models. J Am Coll Cardiol 1993;22:271–6.
28. Redaelli A, Maisano F, Schreuder JJ, Montevecchi FM. Ventricular motion during the ejection phase: a computational analysis. J Appl Physiol 2000;89:314–22.
29. Tsujino H, Jones M, Shiota T, et al. Real-time three-dimensional color Doppler echocardiography for characterizing the spatial velocity distribution and quantifying the peak flow rate in the left ventricular outflow tract. Ultrasound Med Biol 2001;27:69–74.